Transportation Infrastructure Geotechnology (2022) 9:117–129
https://doi.org/10.1007/s40515-021-00216-0

TECHNICAL PAPER

Discussion: The Impact of Variation of Gypsum and Water Content on the Engineering Properties of Expansive Soil [DOI: 10.1007/s40515-021–00192-5]

Amin Soltani[1] · **Duc Thai Duong Nguyen**[2] · **Brendan C. O'Kelly**[3]

Accepted: 25 November 2021 / Published online: 21 January 2022

1 Introduction

Recently, Dutta and Yadav (2021) reported on the effects of gypsum treatment — considering gypsum content (defined as the gypsum-to-soil dry mass ratio with $G=0$, 2, 4, 6, 8, and 10%) and curing period (with $C_P=0$, 1, 7, and 28 days) — on the consistency limits, compactability, and unconfined compressive strength (UCS) of a calcium bentonite soil. In their investigation, test specimens were prepared at three different water content levels or compaction states of $w_{opt}-3\%$, w_{opt}, and $w_{opt}+3\%$ (where $w_{opt}=$ optimum water content (OWC)) for each of the bentonite–gypsum mixtures using a mini-compaction test/device developed by Sridharan and Sivapullaiah (2005) and then tested for UCS. A notable portion of the Dutta and Yadav (2021) paper is dedicated to the development (and validation) of multivariable regression models for the UCS of the investigated bentonite–gypsum mixtures mobilized at the imparted compaction energy level. For the three water content

✉ Amin Soltani
a.soltani@federation.edu.au

Duc Thai Duong Nguyen
ducthaiduongnguyen@students.federation.edu.au

Brendan C. O'Kelly
bokelly@tcd.ie

[1] School of Engineering, IT and Physical Sciences, Federation University, Churchill, VIC 3842, Australia

[2] School of Engineering, IT and Physical Sciences, Federation University, Mount Helen, VIC 3350, Australia

[3] Department of Civil, Structural and Environmental Engineering, Trinity College Dublin, Dublin D02 PN40, Ireland

levels of $w_{opt}-3\%$, w_{opt}, and $w_{opt}+3\%$ they investigated, the following models were proposed:

$$\textbf{For } w_{opt}-3\%: \ \mathrm{UCS} = \exp\left(0.0239 \times G + 0.0662 \times C_P + 0.4680 \times \gamma_{dmax} + 3.4319 \times I_L\right) \quad (1)$$

$$\textbf{For } w_{opt}: \ \mathrm{UCS} = \exp\left(0.07872 \times C_P + 0.49212 \times \gamma_{dmax} + 7.4790 \times I_L\right) \quad (2)$$

$$\textbf{For } w_{opt}+3\%: \ \mathrm{UCS} = \exp\left(0.08746 \times C_P + 0.47952 \times \gamma_{dmax} + 8.6403 \times I_L\right) \quad (3)$$

where G = gypsum content, defined as the gypsum-to-bentonite dry mass ratio (in %); C_P = curing period (in days); I_L = liquidity index, defined by Dutta and Yadav (2021) based on the OWC of the bentonite–gypsum mixture as $I_L = (w_{opt} - w_P)/(w_L - w_P)$ (with w_P and w_L denoting the plastic and liquid limits for each bentonite–gypsum mixture, respectively); and γ_{dmax} = maximum dry unit weight (MDUW) of the bentonite–gypsum mixture (in kN/m^3). Note: From the authors' reanalysis of modeling experimental data presented in the Dutta and Yadav (2021) paper, a typo was discovered in the UCS equation for $w_{opt}-3\%$; the correct version of this relationship being shown as Eq. 1 in the present discussion article (i.e., the coefficient on γ_{dmax} was reported as 0.0468 in the Dutta and Yadav (2021) paper).

In the present discussion article, some apparent shortcomings and limitations associated with the regression models (presented above as Eqs. 1–3) proposed by Dutta and Yadav (2021), as well as some noted inconsistencies in their experimental results and data interpretations, are scrutinized. For instance, the models given by Eqs. 1–3 are counterintuitive from the viewpoint that the UCS correlates positively with (i.e., being directly proportional to) I_L; the opposite being the case in soil mechanics practice. Also, while Eq. 1 considers the gypsum content G, the models given by Eqs. 2 and 3 do not include gypsum content as an input, explained by Dutta and Yadav (2021) as attributed to the t_{ratio} values (which were not reported in their Table 5) not being greater than the corresponding $t_{critical}$ values. This seems unusual from the viewpoint that one is modeling the improvement in UCS arising from G = 0–10% gypsum additive for curing periods of C_P = 1–28 days. As a way forward, new and improved multivariable regression models are introduced (and validated) by the authors of the present article to complement the original experimental results reported by Dutta and Yadav (2021).

2 Reappraisal of the Dutta and Yadav (2021) Regression Models

This section discusses the shortcomings associated with the regression models (Eqs. 1–3) proposed by Dutta and Yadav (2021), taking into consideration the suitability of their selected input/independent variables, the practicality of their proposed models, and, most importantly, the accuracy of the UCS predictions made by their models.

2.1 Suitability of the Selected Input/Independent Variables

Deriving a multivariable regression model that accounts for all variables governing a physical problem, the UCS of compacted bentonite–gypsum mixtures in this case, is a formidable task. In general, a suitable input/independent variable is characterized as one that is not only statistically significant (by exhibiting a high degree of correlation with the output/dependent variable), but also, more importantly, holds physical meaning. Referring to Eqs. 1–3, Dutta and Yadav (2021) employ the gypsum content G, curing period C_P, MDUW γ_{dmax}, and liquidity index I_L as their input variables. While these parameters all appear to be strongly correlated with the UCS, in their currently defined forms, the γ_{dmax} and I_L parameters are not physically meaningful.

In other words, if the I_L parameter is to be used as a UCS predictor, it should be defined based on the actual molding water content of the bentonite–gypsum sample. However, Dutta and Yadav (2021) state that "for the determination of I_L, the w_{opt} of mixtures were taken as natural water content." Clearly, this I_L definition — inferred as $I_L = (w_{opt} - w_P)/(w_L - w_P)$ — is valid/applicable only for those bentonite–gypsum blends compacted at their respective OWC (as is the case in the derivation of Eq. 2). In other words, for the I_L parameter to be a physically meaningful input variable for Eqs. 1 and 3, it needs to be redefined based on the actual water content states of $w_{opt} - 3\%$ and $w_{opt} + 3\%$ as $I_L = [(w_{opt} - 3\%) - w_P]/(w_L - w_P)$ and $I_L = [(w_{opt} + 3\%) - w_P]/(w_L - w_P)$, respectively.

Dutta and Yadav (2021) state that "the cylinder specimens of 76-mm height and 38-mm diameter of bentonite–gypsum mixtures were prepared at three different water content ($w_{opt} - 3\%$, w_{opt}, and $w_{opt} + 3\%$) as per IS 2720 (Part 10) (IS 2720–10 1991) to determine the UCS." While this description does not provide a clear picture of the samples' compaction state in terms of their dry unit weight, it would appear that each bentonite–gypsum mixture has been compacted to a dry unit weight corresponding to either $w_{opt} - 3\%$, w_{opt}, or $w_{opt} + 3\%$ (i.e., $\gamma_{d(-3\%)}$, γ_{dmax}, and $\gamma_{d(+3\%)}$) deduced from its respective compaction curve. This is evidenced by the fact that the ($w_{opt} + 3\%$, γ_{dmax}) molding state would produce an impossible (physically meaningless) compaction condition exceeding the zero-air-voids (ZAV) saturation line (see Fig. 1 of this discussion article). Furthermore, as demonstrated in Fig. 1, it is noted that the compaction states (w_{opt}, γ_{dmax}) and ($w_{opt} - 3\%$, γ_{dmax}) also exceed the ZAV line; it would be appreciated if the (original) authors can provide some clarification on these inconsistencies. In view of the above observations, the use of γ_{dmax} as a UCS predictor is valid/applicable only for those bentonite–gypsum mixtures compacted at their respective OWC (i.e., Eq. 2). In other words, for Eqs. 1 and 3, γ_{dmax} has no physical meaning, as it does not represent the actual compaction states (or dry unit weights) of the samples. If dry unit weight is to be considered a physically meaningful predictor for Eqs. 1 and 3, it needs to be redefined as ($w_{opt} - 3\%$, $\gamma_{d(-3\%)}$) and ($w_{opt} + 3\%$, $\gamma_{d(+3\%)}$), respectively.

Note that, in determining the specific gravity magnitude of each bentonite–gypsum mixture (necessary for calculation of the degree of saturation S_R values presented in Fig. 1), the weighted averaging technique was adopted as follows (Mir and Sridharan 2013; Soltani et al. 2021):

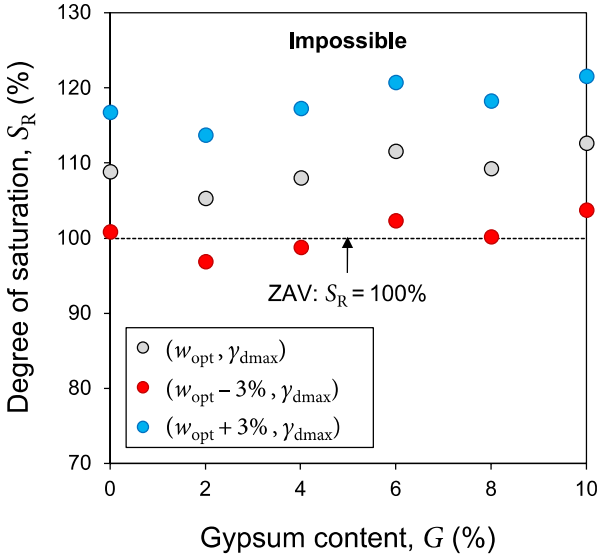

Fig. 1 Variations of degree of saturation S_R against gypsum content G for various compaction states. Note: The OWC and MDUW values used for deducing the S_R parameter were taken from Fig. 3b of Dutta and Yadav (2021)

$$G_s^{BG} = \frac{G_s^B G_s^G (1+G)}{G_s^B G + G_s^G} \tag{4}$$

where G_s^{BG} = specific gravity of the bentonite–gypsum mixture; G_s^B and G_s^G = specific gravity of bentonite (reported as 2.30) and gypsum (reported as 2.41), respectively; and G = gypsum content (i.e., gypsum-to-bentonite dry mass ratio). Note: Considering the possibility of $G_s^B = 2.41$ and $G_s^G = 2.30$ being instead the correct specific gravity values, the compaction state (w_{opt}, γ_{dmax}) still exceeds the ZAV line.

2.2 Practicality of the Proposed Regression Models

A practical regression model can be defined as one that involves a minimal number of readily measurable "independent" variables (as inputs) linked together by a simple functional expression containing a limited number of fitting/model parameters (Zhang et al. 2019; Soltani et al. 2020). In its current form, Eq. 1 contains a total of four fitting parameters; as such, having established the compaction curves (and hence the OWC and MDUW parameters) of the desired bentonite–gypsum mixtures, a minimum of four UCS, four w_L, and four w_P measurements (for four different G–C_P levels) would be required for its calibration. Similarly, calibrating Eqs. 2 and 3, each having three fitting parameters, would involve a minimum of three UCS, three w_L, and three w_P measurements. In the authors' view, the proposed regression models suffer from sophisticated calibration procedures, and thus they would not be trivial to implement in practice.

Furthermore, to avoid potential "multicollinearity" issues, it is critical that the input variables selected for model development remain "independent" — that is, the input variables should (generally) not be strongly correlated with each other

(Farrar and Glauber 1967; McClendon 2002). Given that the γ_{dmax} and I_L parameters themselves are functions of the gypsum content and curing period, as demonstrated in Figs. 3 and 4 of the Dutta and Yadav (2021) paper (i.e., $\gamma_{dmax}=f_1(G)$ and $I_L=f_2(G,C_P)$), their inclusion in the regression analysis may likely lead to multicollinearity issues, producing misleading R^2 and p-value parameters likely unable to reflect the (true) accuracy of the predictions (Daoud 2017). If a suitable functional expression is considered for UCS $=f(G,C_P)$, the gypsum content and curing period should be able to effectively capture the UCS variations (for each of the three compaction states investigated by Dutta and Yadav (2021)); this aspect is further explored in Sect. 3.

2.3 The Need to Critically Examine the Prediction Residuals

It is well established that the sole use of the R^2 statistic, despite being close to unity as demonstrated from reported values in Tables 4 and 6 of the Dutta and Yadav (2021) paper, is not sufficient (nor a reliable basis) to derive firm conclusions about the predictive performance of a multivariable regression model (Vardanega and Haigh 2014; O'Kelly and Soltani 2021; Soltani and O'Kelly 2021a). In other words, for the predictions to be considered reliable, the regression model needs to maintain a certain balance between its goodness-of-fit and its prediction error (Soltani et al. 2020; Soltani and O'Kelly 2022). The goodness-of-fit is routinely evaluated by the R^2 statistic. The prediction error, which has not been taken into consideration in the modeling by Dutta and Yadav (2021), is often examined by means of dimensionless error-related statistics, including the *normalized root-mean-squared error* (NRMSE) and the *mean absolute percentage error* (MAPE), with values closer to 0 indicative of a lower average deviation between the predicted and measured data.

While high R^2 (close to unity) and low NRMSE or MAPE values (close to 0) would normally lead to confirming a model's predictive capability, a critical examination of the model's prediction residuals should also be performed to (at least) better understand the true implications of its predictions for practical geoengineering applications (Soltani et al. 2021). This aspect becomes particularly important for the Dutta and Yadav (2021) investigation, since the R^2, NRMSE, and MAPE parameters are average metrics, which, by definition, are strongly dependent on the database size used for performing the regression analysis. In other words, these fit-measure indices can be strongly biased when dealing with datasets that have been artificially enlarged by inclusion of replicates in the analysis (as practiced by Dutta and Yadav (2021)), often producing misleadingly high R^2 and/or low NRMSE/MAPE values, even though such results do not necessarily reflect the (true) accuracy of the predictions. To ensure that the UCS predictions made by Eqs. 1–3 are indeed acceptable, it is necessary that the upper and lower "statistical limits of agreement" between the predicted and measured UCS values be determined and critically examined; this can be achieved by the Bland–Altman (BA) analysis (e.g., Rehman et al. 2020; Soltani and O'Kelly 2021b). Given that the critical requirements (for the prediction error) mentioned above have not been taken into consideration in the Dutta and Yadav

(2021) investigation, an attempt is made by the authors of this discussion article to assess the prediction errors of the proposed UCS models given by Eqs. 1–3. For the problem at hand, the NRMSE and MAPE (both dimensionless parameters expressed in percentage) can be defined as follows (Soltani and O'Kelly 2022):

$$\text{NRMSE} = \frac{\text{RMSE}}{\frac{1}{N}\sum_{n=1}^{N} \text{UCS}_{\text{M}(n)}} \times 100\% \tag{5}$$

$$\text{RMSE} = \sqrt{\frac{1}{N}\sum_{n=1}^{N} \left(\text{UCS}_{\text{M}(n)} - \text{UCS}_{\text{P}(n)}\right)^2} \tag{6}$$

$$\text{MAPE} = \frac{1}{N}\sum_{n=1}^{N} \left| \frac{\text{UCS}_{\text{M}(n)} - \text{UCS}_{\text{P}(n)}}{\text{UCS}_{\text{M}(n)}} \right| \times 100\% \tag{7}$$

where RMSE = root-mean-squared error (in the same unit as the UCS); UCS_{M} and UCS_{P} = measured and predicted UCS, respectively; n = index of summation; and N = total number of observations/predictions.

Following the BA method, the 95% upper and lower statistical limits of agreement between the predicted and measured UCS values can be obtained as follows (Bland and Altman 1999):

$$\text{UAL}_{95\%} = \mu_{\text{D}} + 1.96 \times \sigma_{\text{D}} \tag{8}$$

$$\text{LAL}_{95\%} = \mu_{\text{D}} - 1.96 \times \sigma_{\text{D}} \tag{9}$$

$$\mu_{\text{D}} = \frac{1}{N}\sum_{n=1}^{N} \left(\text{UCS}_{\text{P}(n)} - \text{UCS}_{\text{M}(n)}\right) \tag{10}$$

$$\sigma_{\text{D}} = \frac{1}{N}\sum_{n=1}^{N} \left(\left(\text{UCS}_{\text{P}(n)} - \text{UCS}_{\text{M}(n)}\right) - \mu_{\text{D}}\right)^2 \tag{11}$$

where $\text{UAL}_{95\%}$ and $\text{LAL}_{95\%}$ = 95% upper and lower statistical limits of agreement, respectively, between the predicted and measured UCS values (in the same unit as the UCS); and μ_{D} and σ_{D} = arithmetic mean and standard deviation of the $(\text{UCS}_{\text{P}} - \text{UCS}_{\text{M}})$ data, respectively.

Making use of the UCS data presented in Fig. 6a (for $w_{\text{opt}} - 3\%$), Fig. 6b (for w_{opt}), and Fig. 6c (for $w_{\text{opt}} + 3\%$) of the Dutta and Yadav (2021) paper, along with the γ_{dmax} and I_{L} values reported in their Figs. 3b and 4c, the respective values of the NRMSE and MAPE parameters can be calculated as 64.8% and 48.2% for Eq. 1, 146.0% and 47.4% for Eq. 2, and 132.0% and 32.1% for Eq. 3. These values, which are significantly higher than the (usual) allowable 5–10% reference limit, indicate an average offset of 32.1–146.0% associated with the

UCS predictions. The 95% upper and lower agreement limits between the predicted and measured UCS values can be calculated as $UAL_{95\%} = +1.22, +3.76$, and +4.03 MPa and $LAL_{95\%} = -0.69, -2.40$, and −2.80 MPa for Eqs. 1, 2, and 3, respectively, indicating that the errors associated with 95% of the predictions made by these equations lie between these two extraordinarily wide stress (UCS) limits. In other words, these wide stress limits cannot be deemed acceptable for UCS prediction purposes.

In the authors' view, given that the variations of the UCS with increasing G and/or C_P (for a given compaction state) are strongly monotonic, as demonstrated in Figs. 6a–c of the Dutta and Yadav (2021) paper, along with the fact that the datasets to be used for developing each regression model are rather small in size ($N = 24$), low NRMSE, MAPE, $UAL_{95\%}$, and $LAL_{95\%}$ values should be easily accomplishable; this is demonstrated in the next section.

3 Proposed Regression Models

In view of the discussions in Sect. 2, for a given compaction state, either $w_{opt} - 3\%$, w_{opt}, or $w_{opt} + 3\%$, the UCS of compacted bentonite–gypsum mixtures can be expressed as follows:

$$\mathrm{UCS} = f\left(G, C_P\right) \tag{12}$$

where f = an unknown multivariable functional expression (to be obtained through trial-and-error).

While an *ad hoc* solution to f is non-existent, the multivariable quadratic function, as given in Eq. 13, has been widely reported as a suitable starting point to initiate the trial-and-error investigation, allowing one to identify statistically significant/meaningful functional terms capable of constructing a practical regression model that is both simple in structure and fairly accurate in terms of its predictions (e.g., Sivakumar Babu et al. 2008; Ahmed 2012; Güllü and Fedakar 2017; Shahbazi et al. 2017; Tran et al. 2018; Soltani and Mirzababaei 2019; Zhang et al. 2019, 2021; Almajed et al. 2021).

$$\mathrm{UCS} = \beta_0 + \beta_1 G + \beta_2 C_P + \beta_3 G^2 + \beta_4 {C_P}^2 + \beta_5 G C_P \tag{13}$$

where β_0–β_5 = fitting/model parameters; and β_0 = UCS of the unamended, uncured compacted bentonite soil, since setting $G = 0$ and $C_P = 0$ results in UCS = β_0. Note that the second-degree terms G^2 and ${C_P}^2$ intend to capture potential nonlinearities between the UCS and the independent variables G and C_P, while the term $G \times C_P$ captures the combined effects of gypsum content and the enacted curing duration.

The proposed regression model given in Eq. 13 was fitted to the measured UCS data (presented in Figs. 6a–c of the Dutta and Yadav (2021) paper) using the conventional least-squares optimization technique. Fisher's F-test was then performed (at $\alpha = 5\%$ significance level) to confirm the models' overall statistical significance, while Student's t-test was conducted (also at $\alpha = 5\%$) to check the statistical significance of the independent regressor terms — that is, G, C_P, G^2, ${C_P}^2$, and $G \times C_P$.

Table 1 Summary of the regression analyses results with respect to Eq. 13

Fit-measure indices

Compaction state	R^2	R^2_{adj}	NRMSE (%)	MAPE (%)	$UAL_{95\%}$ (MPa)	$LAL_{95\%}$ (MPa)	F-value	p-value
$w_{opt}-3\%$	0.998	0.997	4.81	6.78	+0.08	−0.08	1473.77	7.45×10^{-23} (<5%) (S)
w_{opt}	0.999	0.998	4.13	9.40	+0.10	−0.10	2562.42	5.18×10^{-25} (<5%) (S)
$w_{opt}+3\%$	0.993	0.991	10.85	16.47	+0.30	−0.30	493.50	1.34×10^{-18} (<5%) (S)

Regression outputs

Compaction state	Variable	Coefficient	SE	t-value	p-value
$w_{opt}-3\%$	Intercept (kPa)	$\beta_0=161.968$	26.350	6.147	8.36×10^{-6} (<5%) (S)
	G (%)	$\beta_1=5.180$	10.160	0.510	6.16×10^{-1} (>5%) (NS)
	C_P (d)	$\beta_2=74.018$	4.848	15.268	9.58×10^{-12} (<5%) (S)
	G^2 (%^{2})	$\beta_3=-0.609$	0.952	−0.640	5.31×10^{-1} (>5%) (NS)
	$C_P{}^2$ (d^2)	$\beta_4=-0.782$	0.159	−4.917	1.11×10^{-4} (<5%) (S)
	$G\times C_P$ (% d)	$\beta_5=3.774$	0.246	15.325	9.00×10^{-12} (<5%) (S)
w_{opt}	Intercept (kPa)	$\beta_0=170.606$	31.105	5.485	3.29×10^{-5} (<5%) (S)
	G (%)	$\beta_1=-8.428$	11.994	−0.703	4.91×10^{-1} (>5%) (NS)
	C_P (d)	$\beta_2=80.640$	5.723	14.092	3.65×10^{-11} (<5%) (S)
	G^2 (%^{2})	$\beta_3=1.353$	1.124	1.204	2.44×10^{-1} (>5%) (NS)
	$C_P{}^2$ (d^2)	$\beta_4=0.545$	0.188	2.902	9.51×10^{-3} (<5%) (S)
	$G\times C_P$ (% d)	$\beta_5=3.001$	0.291	10.324	5.45×10^{-9} (<5%) (S)
$w_{opt}+3\%$	Intercept (kPa)	$\beta_0=290.002$	91.087	3.184	5.14×10^{-3} (<5%) (S)
	G (%)	$\beta_1=-56.422$	35.123	−1.606	1.26×10^{-1} (>5%) (NS)
	C_P (d)	$\beta_2=60.918$	16.758	3.635	1.89×10^{-3} (<5%) (S)
	G^2 (%^{2})	$\beta_3=4.780$	3.290	1.453	1.63×10^{-1} (>5%) (NS)
	$C_P{}^2$ (d^2)	$\beta_4=1.471$	0.550	2.675	1.54×10^{-2} (<5%) (S)
	$G\times C_P$ (% d)	$\beta_5=7.443$	0.851	8.744	6.75×10^{-8} (<5%) (S)

SE, standard error

(S)Significant

(NS)Not significant

Moreover, the R^2, NRMSE, MAPE, $UAL_{95\%}$, and $LAL_{95\%}$ parameters were calculated to critically examine the new models' predictive capabilities.

The regression analysis results with respect to Eq. 13 are presented in Table 1. For the three compaction states of $w_{opt}-3\%$, w_{opt}, and $w_{opt}+3\%$, the high R^2 (=0.998, 0.999, and 0.993) and low NRMSE (=4.81%, 4.13%, and 10.85%) and/or MAPE (=6.78%, 9.40%, and 16.47%) values confirm the strong agreement between the measured and predicted UCS data, both in terms of correlation and forecast error. While the *p*-values associated with Fisher's *F*-test were all less than 5% (hence confirming the models' overall statistical significance), for all three compaction states the regressor terms G and G^2 produced *p*-values (for Student's *t*-test) greater than 5%, indicating that these two terms are not statistically significant and hence they may have no or little contribution towards the UCS predictions. Insignificant regressor terms are normally eliminated to accommodate the development of a more simplified model (with possibly improved predictions); however, removing both G and G^2 implies that, for $C_P=0$, changes in the gypsum content would consistently produce the same UCS of β_0, even though the experimental data clearly indicate that the UCS increases with increasing gypsum content. This inconsistency can be attributed to the relative impacts of G and C_P on the UCS parameter, with the curing period having a significantly higher impact (or contribution) compared to that of the gypsum content for the 28-day curing period investigated in the Dutta and Yadav (2021) study. In such cases, maintaining physically meaningful predictions takes precedence over statistical significance. Accordingly, to ensure the production of physically meaningful UCS predictions for $C_P=0$, either G or G^2 should be maintained. Given that the *p*-values for G^2 are mainly lower than those obtained for G (refer to Table 1), it was decided to eliminate G, thereby leading to the following simplified models:

$$\textbf{For } w_{opt}-3\%: \quad UCS = 171.201 + 73.881 \times C_P - 0.154 \times G^2 - 0.782 \times C_P{}^2 + 3.801 \times GC_P \tag{14}$$

$$\textbf{For } w_{opt}: \quad UCS = 155.584 + 80.863 \times C_P + 0.614 \times G^2 + 0.545 \times C_P{}^2 + 2.956 \times GC_P \tag{15}$$

$$\textbf{For } w_{opt}+3\%: \quad UCS = 189.440 + 62.409 \times C_P - 0.171 \times G^2 + 1.471 \times C_P{}^2 + 7.145 \times GC_P \tag{16}$$

Like Eqs. 1–3 developed by Dutta and Yadav (2021), the improved Eqs. 14–16 are strictly valid only for the particular calcium bentonite–gypsum mixtures investigated in the domain of $G=0$–10% and $C_P=0$–28 days, and also for the compactive energy level (computed as ~ 1487 kJ/m^3 from the details of the compaction test reported in Dutta and Yadav (2021)) employed in preparing the test specimens for UCS testing.

In terms of graphical representation, Eqs. 14–16 resemble curved surfaces in the three-dimensional space of UCS:G:C_P (see Fig. 2). As for their predictive performance, the NRMSE and MAPE were calculated as 4.84% and 7.14% for Eq. 14 ($w_{opt}-3\%$), 4.18% and 8.56% for Eq. 15 (w_{opt}), and 10.85% and 9.69% for Eq. 16 ($w_{opt}+3\%$), respectively, all of which strongly outperform those deduced for Eqs. 1–3 proposed by Dutta and Yadav (2021). Furthermore, for Eqs. 14–16, the 95% upper and

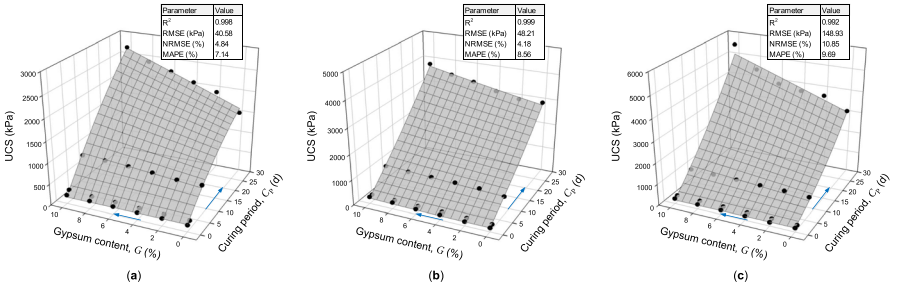

Fig. 2 Graphical representation of the newly proposed Eqs. 14–16 in the three-dimensional space of UCS:G:C_P considering (**a**) $w_{opt}-3\%$, (**b**) w_{opt}, and (**c**) $w_{opt}+3\%$

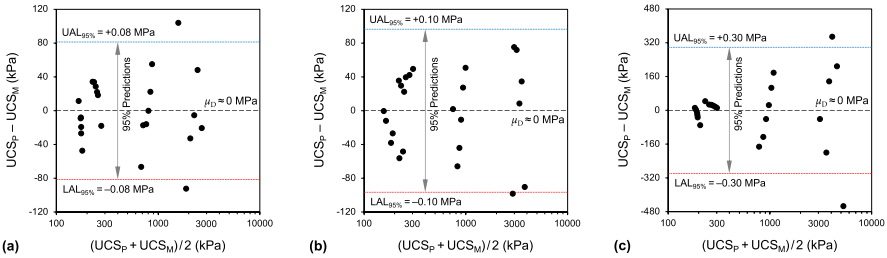

Fig. 3 Bland–Altman plots for the predictions made by (**a**) Eq. 14 ($w_{opt}-3\%$), (**b**) Eq. 15 (w_{opt}), and (**c**) Eq. 16 ($w_{opt}+3\%$). Note: $UAL_{95\%}$ and $LAL_{95\%}$ denote the 95% upper and lower statistical agreement limits, respectively

lower agreement limits between the predicted and measured UCS data were found to be symmetrical (see Fig. 3) and they were calculated as $UAL_{95\%}=+0.08,+0.10$, and $+0.30$ MPa, and $LAL_{95\%}=-0.08,-0.10$, and -0.30 MPa for Eqs. 14, 15, and 16, respectively, indicating that the errors associated with 95% of the predictions made by these new equations lie between these relatively small (and hence acceptable) upper and lower stress (UCS) limits. In terms of practicality, having established the UCS of the unamended, uncured compacted bentonite soil ($G=0$ and $C_P=0$) for $w_{opt}-3\%$, w_{opt}, and $w_{opt}+3\%$, each of the newly proposed equations (Eqs. 14–16) can be calibrated by conducting a total of four additional UCS tests (for four arbitrary G–C_P levels). For a detailed discussion on selecting appropriate mix designs for model calibration (the four G–C_P levels in this case), the reader is referred to the papers by Mirzababaei et al. (2018) and Soltani et al. (2020).

Having confirmed the accuracy of the predictions, Eqs. 14–16 can now be used to perform sensitivity analyses to quantify the relative impacts of the independent variables G and C_P on the UCS, thereby complementing the experimental results reported in the Dutta and Yadav (2021) paper. The relative impact of an independent variable $x_m=G$ or C_P on the dependent variable $y=$UCS can be expressed as follows (Gandomi et al. 2013; Estabragh et al. 2016; Tran et al. 2018):

Table 2 Summary of the sensitivity analyses results with respect to the newly proposed Eqs. 14–16

Compaction state	Independent variable x_m	$d(x_m)$ (kPa)	$S(x_m)$ (%)
$w_{opt}-3\%$	$G=0, 2, 4, 6, 8, 10\%$ ($\overline{G}=5\%$)	326.68	14
	$C_P=0, 1, 7, 28$ d ($\overline{C_P}=9$ d)	1987.69	86
w_{opt}	$G=0, 2, 4, 6, 8, 10\%$ ($\overline{G}=5\%$)	327.42	10
	$C_P=0, 1, 7, 28$ d ($\overline{C_P}=9$ d)	3105.18	90
$w_{opt}+3\%$	$G=0, 2, 4, 6, 8, 10\%$ ($\overline{G}=5\%$)	625.89	14
	$C_P=0, 1, 7, 28$ d ($\overline{C_P}=9$ d)	3900.87	86

$$S(x_m)=\frac{d(x_m)}{\sum_{m=1}^{M} d(x_m)}\times 100\% \tag{17}$$

$$d(x_m)=y_{max}(x_m)-y_{min}(x_m) \tag{18}$$

where $d(x_m)$ = overall relative impact of $x_m = G$ or C_P on y = UCS (in the same unit as the UCS); $S(x_m)$ = percentage contribution provided by $x_m = G$ or C_P towards the y = UCS development (in %); and $y_{max}(x_m)$ and $y_{min}(x_m)$ = maximum and minimum y (= UCS) over the m^{th} input domain, calculated by Eqs. 14–16, where the other input variable is kept constant by setting it equal to its mean value — that is, either (G = 0–10% and $\overline{C_P}=9$ days) or (G = 5% and C_P = 0–28 days).

The sensitivity analysis results with respect to Eqs. 14–16 are summarized in Table 2. In line with the experimental results, for all three compaction states, the contribution to UCS development provided by the curing period (i.e., $S(C_P)$ = 86%, 90%, and 86%) was found to be significantly greater than that provided by the gypsum content (i.e., $S(G)$ = 14%, 10%, and 14%). The individual sensitivities were calculated as $d(G)$ = 326.68, 327.42, and 625.89 kPa, and $d(C_P)$ = 1987.69, 3105.18, and 3900.87 kPa for Eqs. 14, 15, and 16, respectively. These results imply that the greater the molding water content (increasing from $w_{opt}-3\%$ to $w_{opt}+3\%$), the higher the contributions of both G and C_P towards the UCS development.

References

Ahmed, A.: Simplified regression model to predict the strength of reinforced sand with waste polystyrene plastic type. Geotech. Geol. Eng. **30**, 963–973 (2012). https://doi.org/10.1007/s10706-012-9519-0

Almajed, A., Srirama, D., Moghal, A.A.B.: Response surface method analysis of chemically stabilized fiber-reinforced soil. Materials **14**, 1535 (2021). https://doi.org/10.3390/ma14061535

Bland, J.M., Altman, D.G.: Measuring agreement in method comparison studies. Stat. Methods Med. Res. **8**, 135–160 (1999). https://doi.org/10.1191/096228099673819272

Daoud, J.I.: Multicollinearity and regression analysis. J. Phys. Conf. Ser. **949**, 012009 (2017). https://doi.org/10.1088/1742-6596/949/1/012009

Dutta, R.K., Yadav, J.S.: The impact of variation of gypsum and water content on the engineering properties of expansive soil. *Transp. Infrastruct. Geotechnol.* **In Press**, (2021).https://doi.org/10.1007/s40515-021-00192-5

Estabragh, A.R., Soltani, A., Javadi, A.A.: Models for predicting the seepage velocity and seepage force in a fiber reinforced silty soil. Comput. Geotech. **75**, 174–181 (2016). https://doi.org/10.1016/j.compgeo.2016.02.002

Farrar, D.E., Glauber, R.R.: Multicollinearity in regression analysis: the problem revisited. Rev. Econ. Stat. **49**, 92–107 (1967). https://doi.org/10.2307/1937887

Gandomi, A.H., Yun, G.J., Alavi, A.H.: An evolutionary approach for modeling of shear strength of RC deep beams. Mater. Struct. **46**, 2109–2119 (2013). https://doi.org/10.1617/s11527-013-0039-z

Güllü, H., Fedakar, H.İ: Response surface methodology for optimization of stabilizer dosage rates of marginal sand stabilized with sludge ash and fiber based on UCS performances. KSCE J. Civ. Eng. **21**, 1717–1727 (2017). https://doi.org/10.1007/s12205-016-0724-x

McClendon, M.J.: Multiple Regression and Causal Analysis. Waveland Press Inc., Prospect Heights, IL, USA (2002). ISBN:9781577662433

Mir, B.A., Sridharan, A.: Physical and compaction behaviour of clay soil–fly ash mixtures. Geotech. Geol. Eng. **31**, 1059–1072 (2013). https://doi.org/10.1007/s10706-013-9632-8

Mirzababaei, M., Mohamed, M., Arulrajah, A., Horpibulsuk, S., Anggraini, V.: Practical approach to predict the shear strength of fibre-reinforced clay. Geosynth. Int. **25**, 50–66 (2018). https://doi.org/10.1680/jgein.17.00033

O'Kelly, B.C., Soltani, A.: Discussion: Determining the plasticity properties of high plastic clays: A new empirical approach [Arab J Geosci (2020) 13(11), 394]. Arab. J. Geosci. **14**, 715 (2021). https://doi.org/10.1007/s12517-021-06757-5

Rehman, H.U., Pouladi, N., Pulido-Moncada, M., Arthur, E.: Repeatability and agreement between methods for determining the Atterberg limits of fine-grained soils. Soil Sci. Soc. Am. J. **84**, 21–30 (2020). https://doi.org/10.1002/saj2.20001

Shahbazi, M., Rowshanzamir, M., Abtahi, S.M., Hejazi, S.M.: Optimization of carpet waste fibers and steel slag particles to reinforce expansive soil using response surface methodology. Appl. Clay Sci. **142**, 185–192 (2017). https://doi.org/10.1016/j.clay.2016.11.027

Sivakumar Babu, G.L., Vasudevan, A.K., Sayida, M.K.: Use of coir fibers for improving the engineering properties of expansive soils. J. Nat. Fibers. **5**, 61–75 (2008). https://doi.org/10.1080/15440470801901522

Soltani, A., Mirzababaei, M.: Discussion of "Compaction and strength behavior of tire crumbles–fly ash mixed with clay" by Akash Priyadarshee, Arvind Kumar, Deepak Gupta, and Pankaj Pushkarna. J. Mater. Civ. Eng. **31**, 07019004 (2019). https://doi.org/10.1061/(asce)mt.1943-5533.0002701

Soltani, A., O'Kelly, B.C.: Reappraisal of the ASTM/AASHTO standard rolling device method for plastic limit determination of fine-grained soils. Geosciences **11**, 247 (2021b). https://doi.org/10.3390/geosciences11060247

Soltani, A., Deng, A., Taheri, A., Mirzababaei, M., Jaksa, M.B.: A dimensional description of the unconfined compressive strength of artificially cemented fine-grained soils. J. Adhes. Sci. Technol. **34**, 1679–1703 (2020). https://doi.org/10.1080/01694243.2020.1717804

Soltani, A., Azimi, M., O'Kelly, B.C.: Modeling the compaction characteristics of fine-grained soils blended with tire-derived aggregates. Sustainability **13**, 7737 (2021). https://doi.org/10.3390/su13147737

Soltani, A., O'Kelly, B.C.: Discussion of "The flow index of clays and its relationship with some basic geotechnical properties" by G. Spagnoli, M. Feinendegen, L. Di Matteo, and D. A. Rubinos, published in Geotechnical Testing Journal 42, no. 6 (2019): 1685–1700. Geotech. Test. J. **44**, 216–219 (2021a). https://doi.org/10.1520/gtj20190423

Soltani, A., O'Kelly, B.C.: Reappraisal of fall-cone flow curve for soil plasticity determinations. *Geotech. Test. J.* **45**, (2022). https://doi.org/10.1520/gtj20200312

Sridharan, A., Sivapullaiah, P.V.: Mini compaction test apparatus for fine grained soils. Geotech. Test. J. **28**, 240–246 (2005). https://doi.org/10.1520/gtj12542

Tran, K.Q., Satomi, T., Takahashi, H.: Improvement of mechanical behavior of cemented soil reinforced with waste cornsilk fibers. Constr. Build. Mater. **178**, 204–210 (2018). https://doi.org/10.1016/j.conbuildmat.2018.05.104

Vardanega, P.J., Haigh, S.K.: The undrained strength–liquidity index relationship. Can. Geotech. J. **51**, 1073–1086 (2014). https://doi.org/10.1139/cgj-2013-0169

Zhang, J., Soltani, A., Deng, A., Jaksa, M.B.: Mechanical performance of jute fiber-reinforced micaceous clay composites treated with ground-granulated blast-furnace slag. Materials. **12**, 576 (2019). https://doi.org/10.3390/ma12040576

Zhang, J., Deng, A., Jaksa, M.: Optimizing micaceous soil stabilization using response surface method. J. Rock Mech. Geotech. Eng. **13**, 212–220 (2021). https://doi.org/10.1016/j.jrmge.2020.05.005